Biophysical Journal, Volume *111*

Supplemental Information

Membrane Anchoring and Ion-Entry Dynamics in P-type ATPase Copper Transport

Christina Grønberg, Oleg Sitsel, Erik Lindahl, Pontus Gourdon, and Magnus Andersson

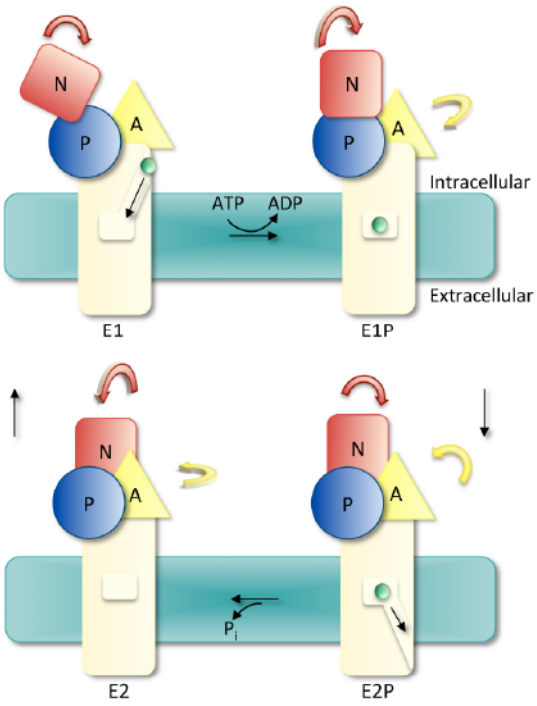

Figure S1. A schematic illustrating the overall E1-E1P-E2P-E2 reaction scheme. The cytosolic domains are shown as in Figure 1 and copper is depicted in green.

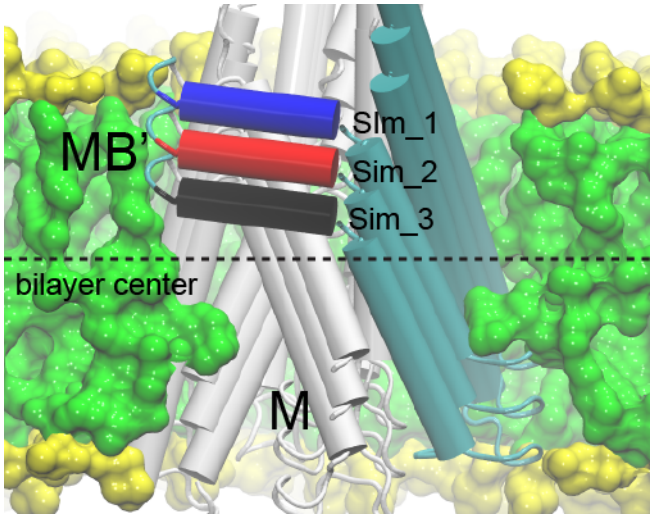

Figure S2. Simulation-system setup. The initial positions of LpCopA relative to the lipid bilayer are shown using different colors for the MB' platform; red for the system that was aligned according to the "Orientations of Proteins in Membranes" (OPM) database (Sim_2), and black and blue for systems inserted 5 Å below (Sim_1) and above (Sim_3) the aligned position.

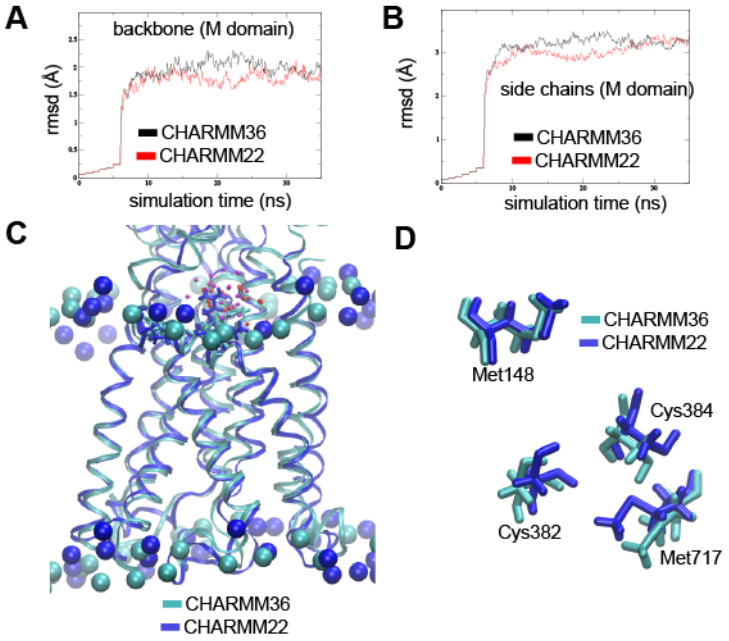

Figure S3. Comparison of simulation dynamics between CHARMM22 and CHARMM36 protein force fields. **(A)** Backbone and **(B)** Side-chain rmsd for the M domain obtained by CHARMM22 (red) and CHARMM36 (black) force fields, respectively. **(C)** Superimposed M domain protein structures corresponding to 35 ns of simulation with the CHARMM22 (blue) and CHARMM36 (cyan) force fields. The proteins are shown in ribbon representation and lipid phosphates are shown as vdW spheres. Platform residues Lys135, Arg136, and Lys142 are shown in licorice and waters within 4 Å from the platform residues are shown in red (CHARMM22) and magenta (CHARMM36). **(D)** Superimposed critical amino acid residues corresponding to 35 ns of simulation with the CHARMM22 (blue) and CHARMM36 (cyan) force field, respectively.

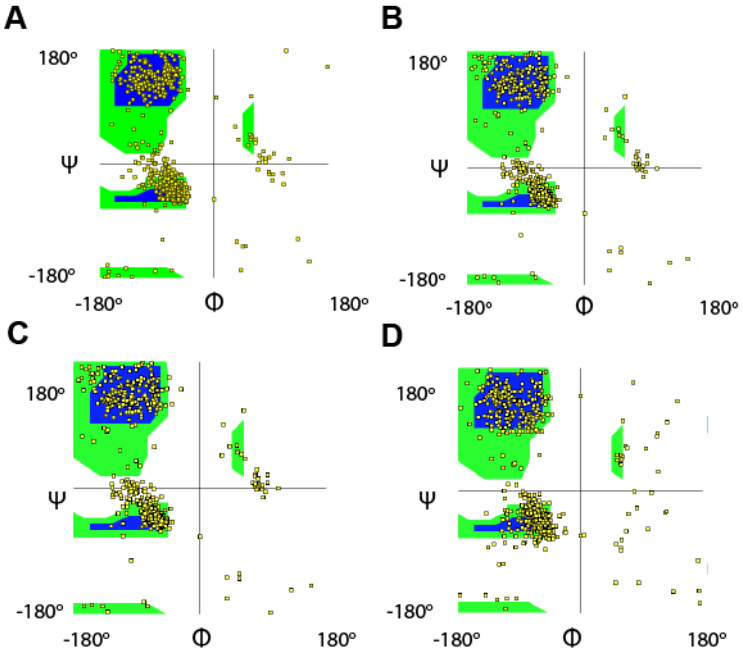

Figure S4. Structural integrity of the E1 model. Ramachandran plots of the **(A)** E2P crystal structure (PDB ID: 4BBJ), **(B)** the E1 model after 10 ns of CHARMM equilibration, **(C)** before and **(D)** after the pull simulation.

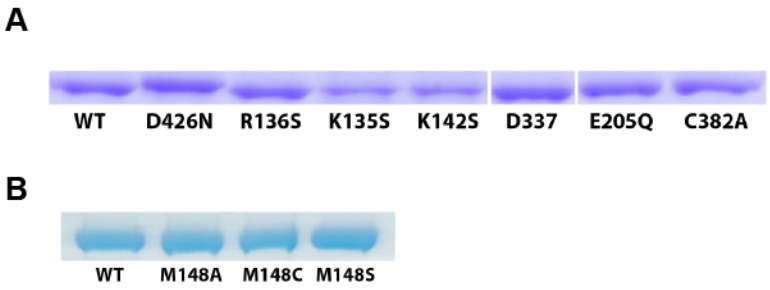

Figure S5. Control SDS-PAGE displaying relative protein concentrations in the *in vitro* functional assays of **(A)** R136S, K135S, K142S, D337N, E205Q, C382A, and **(D)** M148A, M148C, and M148S.

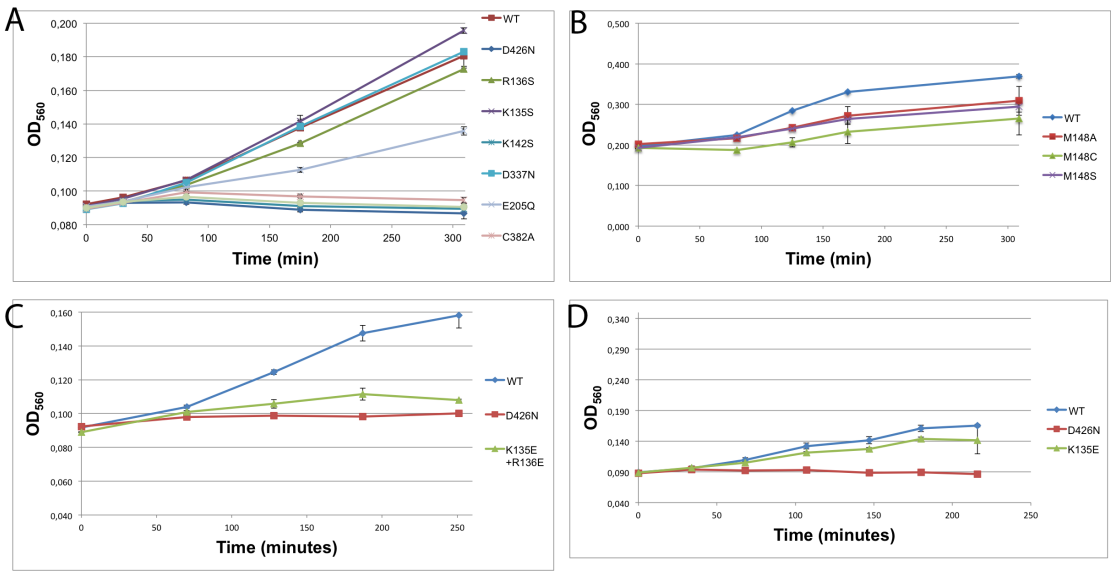

Figure S6. *In vivo* functional assays. Growth curves of wild-type and mutant LpCopA **(A)** D426N, R136S, K135S, K142S, D337N, E205Q, C382A **(B)** M148A, M148C, M148S **(C)** D426N, K135E+R136E **(D)** D426N, K135E in supplemented *E. coli* cells deficient in native CopA. The $CuCl_2$ concentration was 3.5 mM.

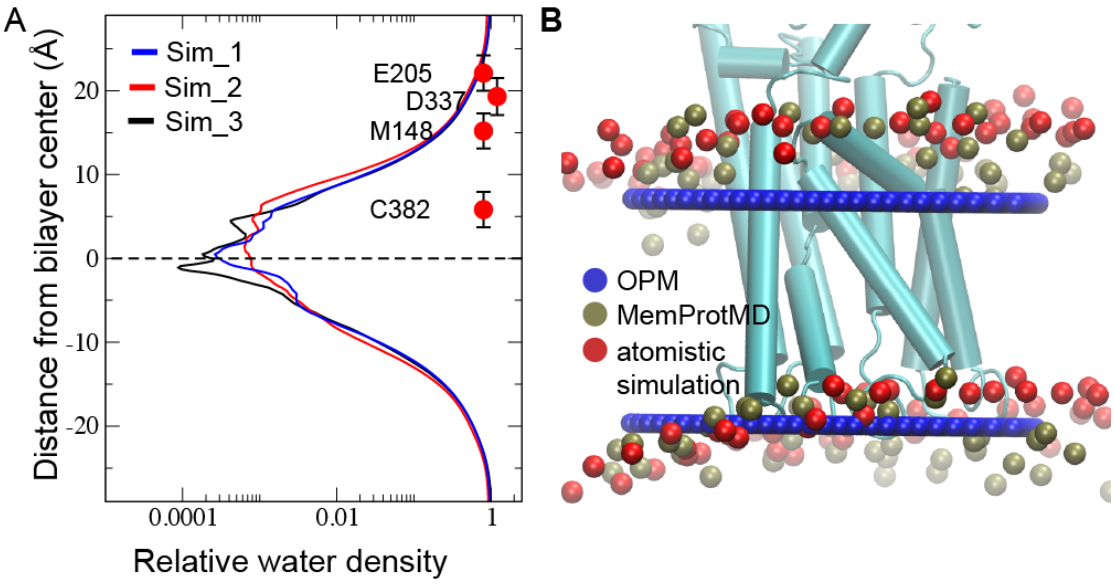

Figure S7. (A) The water density profiles for the converged part (>150 ns) of the three simulations and merged COM for the putative entry site triplet (Met148, Glu205 and Asp337) and internal site residue (Cys382). **(B)** Comparison of membrane insertion of LpCopA (cyan) using the "Orientations of Proteins in Membranes" (OPM) database (blue vDW patches), the MemProtMD database (lipid phosphates show in brown), and our atomistic simulation approach (lipid phosphates shown in red).

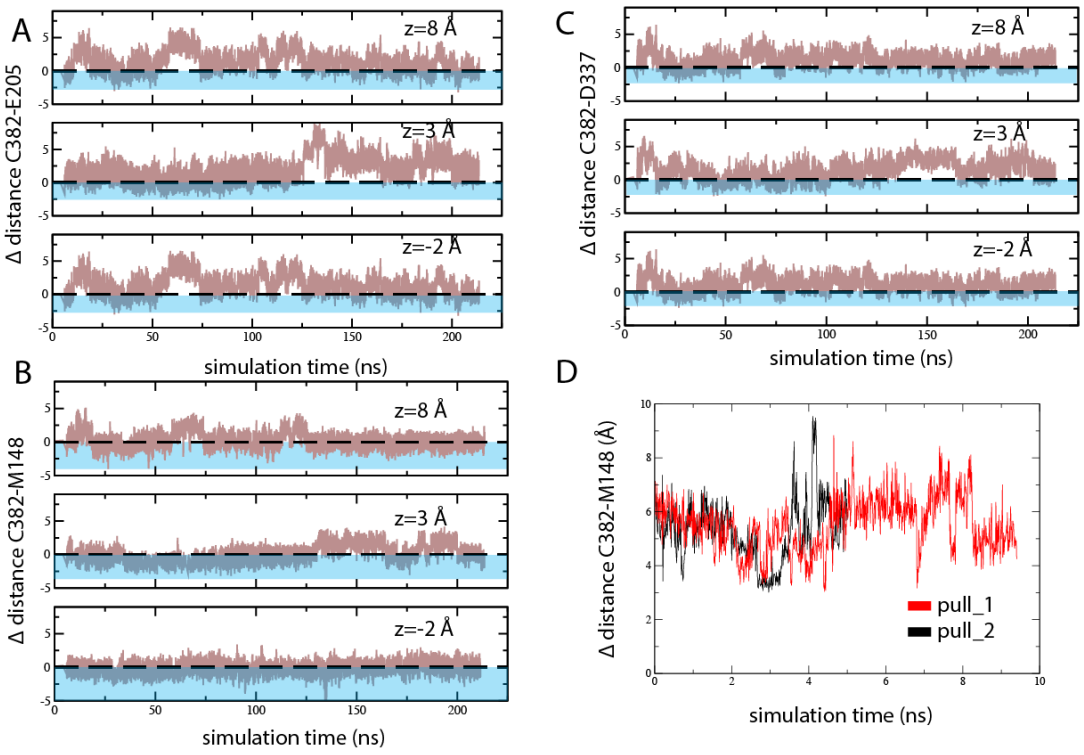

Figure S8. Inter-residue distances between Cys382 and **(A)** Glu205, **(B)** Met148, **(C)** Asp337 relative to the crystal structure distances (zero, dashed lines) for the three simulations; Sim_1, Sim_2, and Sim_3. The blue sections denote the distance range < crystal structure distance. **(D)** Inter-residue distances between Cys382 and Met148 in the simulations of the E1 state in the presence of Cu^{+}.

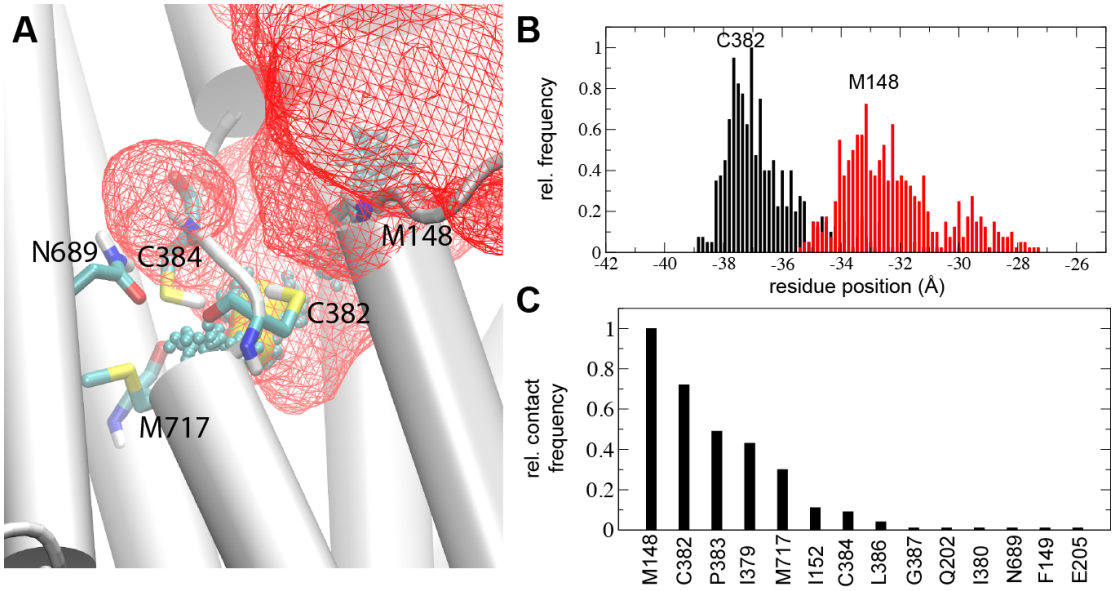

Figure S9. Water and Cu^{+} dynamics. **(A)** Water molecules within 10 Å of Met148 extracted from the 100 ns gromos simulation are shown as a red mesh isodensity surface at 5 % occupancy. **(B)** Structural rearrangements of Met148 and Cys382 side chains in the presence of Cu^{+} depicted as center-of-mass (COM) fluctuations in the pull_2 simulation. **(B)** Contact analysis showing the relative number of instances the Cu^{+} was < 3.5 Å from any protein residue during the pull_2 simulation.

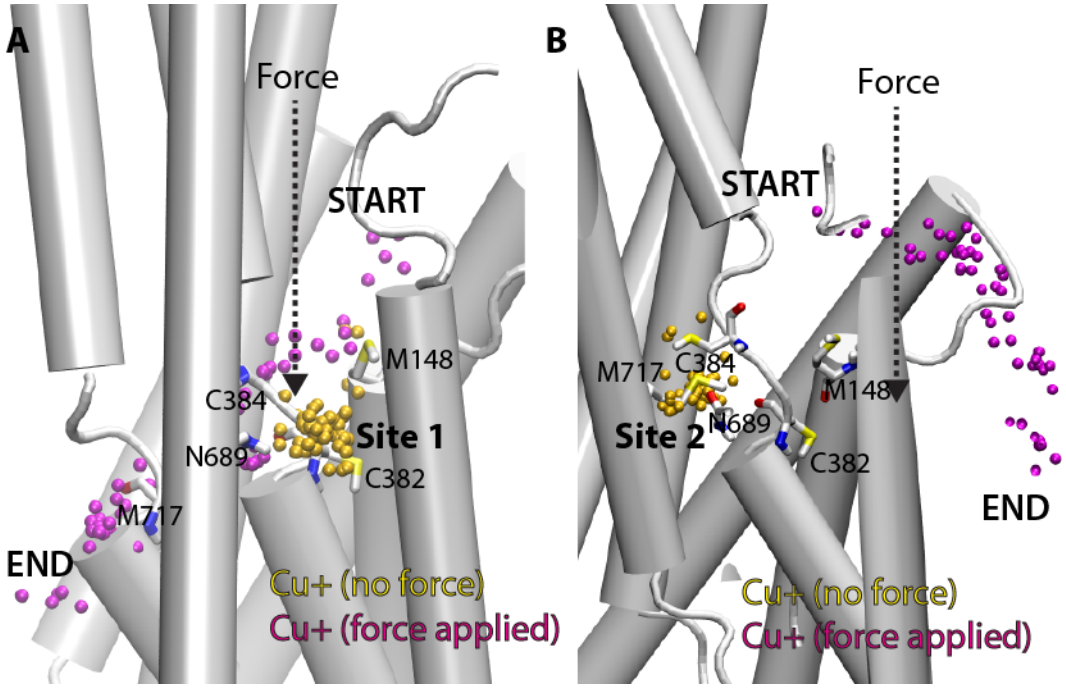

Figure S10. Simulations addressing a putative two-ion Cu^{+} entry. **(A)** A Cu^{+} ion with a starting position in-between residues Met148 and Cys382 (Site 1) was simulated without applied external force (yellow). A starting position for the second Cu^{+} ion (magenta) was chosen vertically aligned to the primary entry site residue Met148 and an external force was applied throughout the simulation. The ion positions correspond to every 1250 ps in a 25000 ps trajectory. **(B)** Similar setup as in (A) with the nonbiased Cu^{+} ion in a starting position proximal to Cys382, Asn689 and Met717 (Site 2).

Simulation	Trajectory lenght (ns)	C382 position along membrane vertical (Å)	M148 position along membrane vertical (Å)	M148-C382 distance (Å)
apo (Sim_1)	210	-36±2	-27±1	9±2
apo (Sim_2)	210	-34±2	-25±2	9±2
apo (Sim_3)	210	-32±2	-23±2	9±2
Cu^+ pull_1 1.25Å/ns	10	-36±1	-31±1	5±1
Cu^+ pull_2 2.5 Å/ns	5	-37±1	-32±1	5±1

Table S1. Simulation lengths, center-of-mass positions of residues Cys382 and Met148, and the corresponding Met148-Cys382 distance.

Simulation (Transient Site occupied)		**Simulation (Internal site occupied)**	
Residue	**Contact time (ns)**	**Residue**	**Contact time (ns)**
Met717	4.28	**Gly144**	3.81
Cys384	3.25	**Thr143**	3.11
Glu205	2.45	**Gln145**	1.30
Phe149	1.99	**Leu146**	0.28
Pro383	1.04	**Asn147**	0.13
Ala714	0.99	**Ser340**	0.8
Leu386	0.88	**Ser140**	0.7
Asn147	0.66	**Leu386**	0.6
Ala718	0.64	**Arg334**	0.3
Gly387	0.62	**Leu335**	0.2

Table S2. Residues within 3.5 Å and contact times of a second docking Cu^{+} during 10 ns steered MD simulations with either the transient Cu^{+} site or the internal Cu^{+} binding site occupied.

Number of Lys and Arg in MB'	Number of sequences
0	1
1	16
2	172
3	265
4	126
5	34
6	3
7	0

Table S3. Number of positively charged residues in the MB' helix of 617 CopA-type proteins with less than 95 % sequence identity selected from the UniProt database were included in the analysis.